IMECE2002-39362

DIE LIFE PREDICTION IN RAPID PROTOTYPE DIES

Young-Bin Park
Georgia Institute of Technology
School of Mechanical Engineering
Atlanta, Georgia 30332-0405 U.S.A.
+1-404-894-3221 (Phone)
+1-404-894-9342 (Fax)
gte640q@prism.gatech.edu

Jonathan S. Colton, Fellow ASME
Georgia Institute of Technology
School of Mechanical Engineering
Atlanta, Georgia 30332-0405 U.S.A.
+1-404-894-7407 (Phone)
+1-404-894-9342 (Fax)
jonathan.colton@me.gatech.edu

ABSTRACT

To meet the growing demand for rapid, low-cost die fabrication technology in the sheet metal forming industry, easy-to-machine, polyurethane-based, composite board stock is used widely as a rapid tooling material. In practice, it is desirable to terminate die life by wear rather than by catastrophic fatigue. However, the failure mechanisms of the rapid prototyped tools are not clearly understood, thus making the prediction of tool life difficult. This paper presents a method to estimate the fatigue life of a sheet metal forming die fabricated from ATH (aluminum trihydrate)-filled polyurethane. A finite element model of 90° V-die bending process was developed, and the effects of process parameters on stress distribution in the punch and die were investigated through simulation. Mechanical testing was performed to characterize the fatigue properties of the tooling material. The computer-simulated results were verified through experiments using instrumented, laboratory-scale punch and die sets.

Keywords: Rapid Tooling, Die Life, Fatigue

INTRODUCTION

Rapid prototype (RP) technology has been drawing attention from the manufacturing industry for more than 10 years. Recent applications of RP technology include rapid tooling (RT), which is the technology that adopts RP techniques in die making. As today's ever-competitive business environment demands reductions in product development time and cost, the need for faster turn-around times and more efficient means of producing prototype and short-run tooling has increased. As a result, RT technology has made inroads into conventional die fabrication methods with the aim of reducing the lead time and investment costs of tooling development.

Despite the fact that sheet metal forming is a widely practiced fabrication process in industry, its exposure to RP and RT technologies have been rather limited. This is due to the general notion that sheet metal forming is suitable for mass production and that it is classified as a two-dimensional process [1]. Because of the planar nature of the workpiece in its initial state, it has been considered inappropriate for RP applications, which often involve three-dimensional solid modeling and implementation of subsequent CAD data. However, the finished sheet metal products are usually three dimensional after undergoing bending and stretching, which qualifies sheet metal forming as a potential candidate for the application of RP techniques. However, as Nakagawa [2] points out, the trend of manufacturing technology is shifting toward small lot production with tighter production schedule, which is triggering the advance in RT technology.

One category of rapid tooling technology involves the application of advanced polymers and composite materials to fabricate sheet metal forming dies. One such material is aluminum trihydrate(ATH)-filled polyurethane, which offers easy handling, fast lead times and low costs while maintaining high-quality standards. Compared with conventional die materials, polyurethane board stock allows high machining rates, which bring about reductions in tooling time and overall production costs [3].

Despite their advantages in terms of lead time and cost, polymer composite dies for sheet metal forming application have several drawbacks. Due to their lack of strength as compared to conventional die materials, the use of polymer composite dies often is limited to prototype or short-run production. Also, because the failure mechanisms are not fully understood, dies are still designed on the basis of the trial-and-error and the experiences of skilled workers, often employing the design rules established for metal dies. These factors often lead to an inappropriate selection of geometry and dimensions, which may result in the premature fatigue failure of the dies.

Unlike polymer composite dies, a number of studies have been performed to analyze the fatigue failure of the die and to achieve better tool design in the case of metal dies – both computationally and experimentally [4-7]. Most of them

involve computer-aided techniques with the common goal of reducing development time and cost by replacing full-scale process trials with simulations. Numerical simulation and modeling of metal forming processes, based on the knowledge of underlying process mechanics and validated by experimental results, provide a powerful tool for optimizing process parameters.

As for sheet metal forming, the formability and failure of sheet metals have been of great interest. Yet, not much attention has been paid to the failure and life prediction of the dies. A study by Jensen *et al.* [8] obtained the distribution of tool wear on the die profile in deep drawing. However, the fatigue life of the die must be considered simultaneously, since it is important to design the tool in such a way that the service life of the tool ends by wear rather than by catastrophic fatigue failure [5].

A different approach is necessary to predict the fatigue life of the polymer composite tool and to optimize tool geometry to enhance tool life. The stress state in the dies must be determined accurately, and the fatigue mechanisms in brittle polymers must be incorporated in the fatigue life prediction method. Ratner and Potapova [9] showed that the maximum principal stresses are the criterion for brittle failure in multicycle fatigue. Suresh [10] documented that cyclic deformation and the subcritical advance of fatigue fracture in many polymers are dictated by the nucleation, growth, and breakdown of crazes, and that the criterion for the nucleation of a craze involves maximum and minimum principal stresses. Ritchie *et al.* [11] reported that the mechanisms of fatigue damage in brittle materials are inherently different from those in metals, and that much future effort must be devoted to the topic.

This paper proposes a general scheme for die life prediction that can be useful to practicing engineers in die-making industry. In particular, a method to estimate the fatigue life of a sheet metal forming die fabricated from ATH-filled polyurethane is presented. First, to establish a fundamental understanding of the nature of the material, engineering data were obtained by characterizing the material in various perspectives. Then, a local stress-based fatigue approach was proposed as the die life estimation method, where the stress levels at critical regions in the die served as the indices for determining the cycles to fatigue failure. Next, on the basis of material data, a finite element method was employed to simulate 90° V-die bending and to obtain the stress distributions in the die. The simulation results were validated through experiments using instrumented, laboratory-scale punch and die sets.

A finite element method also was used to investigate the effects of process parameters on the fatigue life of the die. The dominant process parameters determined from the parameter study can be used in the design stage to effectively control the stress level in the die, and thus the resistance to crack initiation.

MATERIAL CHARACTERIZATION

Composition

This paper deals with a polymer composite tooling material specially developed for metal forming applications known as Ren Shape 5166 by Vantico Inc. The material has a thermosetting polyurethane base, filled with aluminum trihydrate (ATH). The spherical ATH is randomly dispersed in the matrix to impart material isotropy and adhesion. More importantly, the ATH particles serve to increase the overall compressive strength and to improve tribological characteristics. Pyrolysis (according to ASTM D 2584) revealed that the content of ATH is 68.7% by weight.

Mechanical Properties and Fracture Behavior

Mechanical tests were performed to identify the tensile and flexural properties of the material according to ASTM D 638 and ASTM D 790, respectively. The results are summarized in Table 1. The linearity of the stress-strain response indicates that the material is brittle and that little plastic deformation takes place before failure. One key characteristic of Ren Shape 5166 is that its compressive strength (86 MPa; manufacturer's data) is significantly higher than its tensile strength (33 MPa; measured data). This qualifies Ren Shape 5166 as an effective tooling material since the dies tend to be subjected to high compressive loads in metal forming.

Table 1 Mechanical properties of Ren Shape 5166

Property		Tested	Manufacturer
Elastic modulus		7.2 GPa	7.2 GPa
Yield strength (0.2% offset)		32 MPa	32 MPa
Ultimate tensile strength		33 MPa	34 MPa
Flexural modulus	3-point	6.8 GPa	6.7 GPa
	4-point	6.2 GPa	N/A
Flexural strength	3-point	62 MPa	55 MPa
	4-point	54 MPa	N/A
Compressive modulus		N/A	5.8 GPa
Compressive strength (0.2% offset)		N/A	86 MPa

The brittle nature of Ren Shape 5166 is further supported by its fracture toughness. Plane strain fracture toughness tests were performed in accordance with ASTM D 5045, and the single-edge-notch bending (SENB) method was employed. The linearity of the load-displacement curves validates the assumption of linear elastic behavior of the cracked specimens. Three replicate tests yielded the critical stress intensity factor K_{Ic} of 2.20 MPa$\sqrt{m}$.

Subsequent fractographic analysis was performed on the fracture surfaces of the SENB specimens to identify the mode of failure. On a macroscopic level, precise matches of the fracture surfaces indicated the absence of significant plastic deformation. The fractographs taken using an optical stereomicroscope (Fig. 1) revealed some key features of the fracture surfaces. The fracture mechanism is dominated by debonding between the ATH particles and the polyurethane matrix. A vast distribution of voids, as well as the sites of debonding over the surfaces, shows that the crack initiated at the razor notch of the SENB specimen and propagated through voids and along filler-matrix interfaces.

Tribological Properties

Lubrication and friction conditions in sheet metal forming are important in lowering forces, increasing drawability, and reducing tool wear. In conventional deep drawing, lubrication is minimized since the friction between the punch and the blank tends to improve drawability. However, the type and the amount of lubrication applied require experience and reference
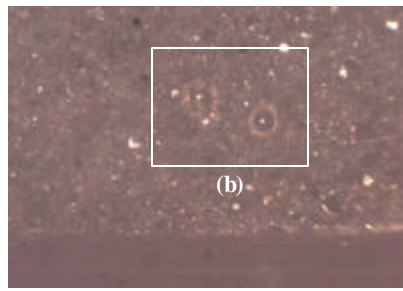
(a) 4X
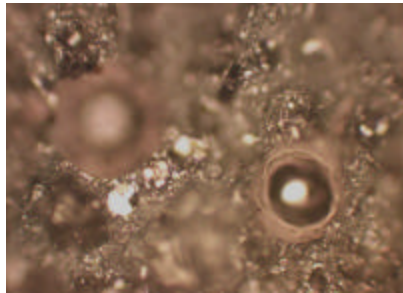
(b) 20X

**Fig. 1 Fractographs of fracture surface
(Ad-Pd sputter coated)**

to engineering data, since excessive friction may result in eventual necking and tearing of the sheet metal.

The polymer composite rapid tooling material is advantageous because it eliminates the need for lubrication. As the material undergoes machining, the polyurethane matrix encapsulates the ATH filler particles. The heat generated during machining creates polyurethane coating over the machined surface and reduces friction. As reported by Tadmor and Gogos [12], in polymer-metal dry friction, both adhesion and ploughing contribute to friction, adhesion usually being the dominant factor. The soft nature of polymers as compared with metals makes the former susceptible to being ploughed. Tadmor and Gogos found that if the adhesive force between the metal and the polymer is greater than the cohesive polymer force, sliding occurs at a plane within the polymer, resulting in the kinematic friction coefficient of greater than 0.2. On the other hand, if the adhesive forces are weaker than the cohesive, sliding occurs at the interface, and the kinematic friction coefficient is less than 0.1. Most polymers fall in the former category. The sliding speed has only moderate effect on the coefficient of friction. An increase in speed tends to increase the friction coefficient. A typical polymer has a kinematic friction coefficient of approximately 0.3 when the speed reaches 10 cm/s.

An experimental setup was designed to measure static friction coefficient between the surfaces of metal sheet and Ren Shape 5166 at room temperature. The coefficients were measured at seven different normal loads, and five replications were made for each load. The polymer sliding blocks were polished to the degree equivalent to an actual die surface, and they were allowed to slide on a 3003-H14 aluminum sheet surface. All contact surfaces were treated with isopropyl alcohol prior to each test to remove contamination and impurities. As the plot in Fig. 2 suggests, static friction coefficient decreases with increasing normal load and becomes constant at high normal loads, with a value of approximately
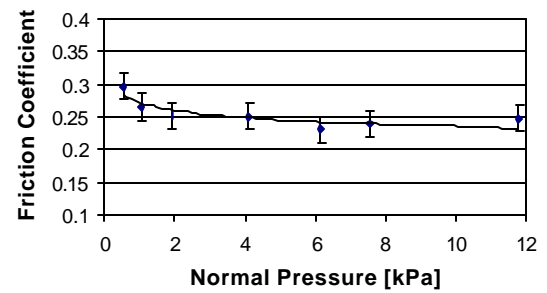
Fig. 2 Friction coefficient versus normal load

0.25. If the adhesive forces at the polymer-metal interface are considered dominant, as is the case with most polymers, the kinematic friction coefficient is typically greater than 0.2 [12]. Since the kinematic friction coefficient can never be greater than the static friction coefficient, the kinematic friction coefficient between Ren Shape 5166 and metal was determined to be 0.2. This value was used in subsequent finite element analyses.

TOOL LIFE PREDICTION METHOD

In metal forming, wear and mechanical fatigue are the competing mechanisms for tool failure. Wear occurs in a gradual, progressive manner and determines the service life of the tool. Therefore, it is critical to design the tool in such a way that tool life is terminated by wear rather than by catastrophic fatigue failure. Accordingly, it becomes an important issue to predict the failure mode and the life of the die. They can provide crucial information and guidelines on die fabrication and part production scheduling, which ultimately influences the overall production time and cost.

During a sheet metal forming process, the deformation of the die takes place mainly in the elastic regime. Therefore, the fatigue mode of the die can be described as high cycle fatigue since the stress amplitude is typically below the yield stress of the material. Moreover, if it is assumed that no cracks pre-exist, the fatigue life is controlled by the number of cycles to crack initiation, and the contribution of crack propagation can be neglected.

In this study, the stress-life (*S-N*) approach is investigated, which is typically used in high cycle fatigue involving constant amplitude loading and negligible plastic strains [13]. One such approach is the local stress-based fatigue approach, based on the assumption that a crack develops at a point that experiences the greatest tensile cyclic loading. One example of such points occurs at the bend region of the die. At the bend region, the stress increases sharply to its maximum value as the punch is bottomed and drops to zero as the punch is retracted. This suggests that the die is subjected to zero-to-tension cyclic loading with the conditions listed in Eq. (1).

$$R = \frac{s_{\min}}{s_{\max}} = 0 \qquad (1a)$$

$$s_m = s_a = \frac{s_{\max}}{2} \qquad (1b)$$

where s_m is the mean stress and s_a is the stress amplitude. Once the stress amplitude is known, the constraint given by Eq.

3 Copyright © 2002 by ASME
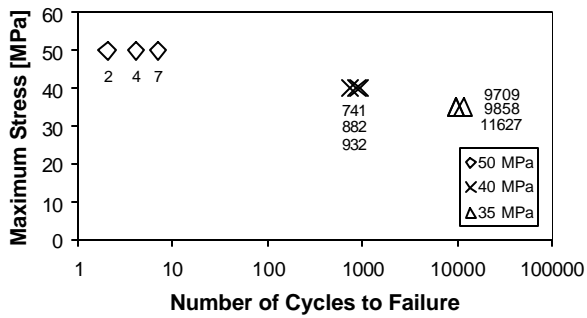
Fig. 3 *S-N* curve from zero-to-tension fatigue tests

(1b) reduces the number of *S-N* curves that are necessary to determine fatigue life to one.

Figure 3 shows the *S-N* data obtained from zero-to-tension fatigue tests for Ren Shape 5166. The tests were performed in four-point flexural test mode with the specimens prepared according to ASTM D 790. The test specimens measured 127 mm by 12.7 mm with a thickness of 3.2 mm. The cyclic loading was strain-controlled, and the loading frequency of 1 Hz was used, which was low enough to minimize hysteretic heating. Three specimens were tested at the maximum tensile stresses of 50, 40, and 35 MPa each. The specimens tested below 35 MPa lasted more than 10^5 cycles, which can be "loosely" interpreted as the endurance limit from the prototype and short-run production viewpoints. The tests were performed up to 10^5 cycles because typically an endurance limit is clearly defined only for plain-carbon or low-alloy steels. In addition, the tests were not limited to shorter numbers of cycles to failure, *e.g.* 100 or 1000 cycles, because there is no reason to limit the application of the tooling material to low volume production if it is capable of producing more parts.

The *S-N* data in Fig. 3 indicate a linear relation between the maximum stress and the life, and it can be expressed as Eq. (2).

$$\textbf{\textit{s}}_{max} = -4.32 \log N_f + 52.50 [\text{MPa}] \qquad (2)$$

Equation (2) yields tool life estimation when the critical point in the die undergoes a zero-to-tension cyclic loading. However, it should be noted that the data (Fig. 3) become scattered as the maximum stress level decreases.

When fatigue test specimens are subjected to bending instead of axial loading, the specimen size effect must be taken into account. The size effect is related to a stress gradient existing in the specimen, which in turn controls the volume of material subjected to the highest levels of stress [14]. For bending, the smaller the size (namely, the cross section) of the specimen, the higher the stress gradient and the smaller the volume of material under maximum stress. Kuguel [15] related the effect of size on fatigue behavior to the volume of the thin layer of surface material subjected to high stresses using Eq. (3)

$$\frac{S_e}{S_{e0}} = \left(\frac{V}{V_0}\right)^{-0.034} \qquad (3)$$

where S_{e0} is the endurance limit for a specimen of volume V_0, and S_e is the endurance limit at some other volume V. The volumes are the portions of the material subjected to at least 95% of the maximum stress.

In V-die bending, the die is subjected to bending around the bend region since the bending force is continuously exerted at two symmetrical points along the 'V' surface. This makes the *S-N* data obtained from bending more appropriate than those from axial testing. Since dies come in various sizes and shapes, the size effect must be considered. If the ratio V/V_0 is close to unity, Eq. (2) is applicable for tool life prediction.

PROCESS SIMULATION

Finite Element Model

A 90° V-die bending process was simulated using the finite element method. A two-dimensional geometric model was constructed using the commercial package ABAQUS/CAE as shown in Fig. 4. Due to symmetry, only half of the model was taken into account. The model consisted of three parts: punch, die, and sheet metal. The punch and the die were modeled as isotropic, elastically deformable bodies with small elastic strains (typically less than 5%) and the mechanical properties of Ren Shape 5166. Elastic modulus E of 7.2 GPa (from tensile tests) and Poisson's ratio $\textbf{\textit{n}}$ of 0.34 (typical for a thermoset) were used. The sheet metal was modeled as elastic and linearly strain-hardening to realistically account for plastic deformation. Plane stress condition (*i.e.,* small thickness) was assumed in order to allow the comparison with experimental results using strain gages, as will be discussed in the following section. Geometric parameters were selected based on the guidelines provided by the die design handbook [16], if applicable. Punch travel distance was determined so that the punch would bottom exactly. Process conditions are summarized in column A of Table 2.

Due to the nonlinear nature of the process, instability in the solution may result. An iterative method was used to determine the optimal mesh density. The mesh size was reduced until solution convergence was reached, localized instability (manifested by chatter in the stress values along the 'V' profile) was eliminated, and further refinement no longer had any significant effect on the stress field. The optimal mesh size along the 'V' surface, where the contact takes place, was
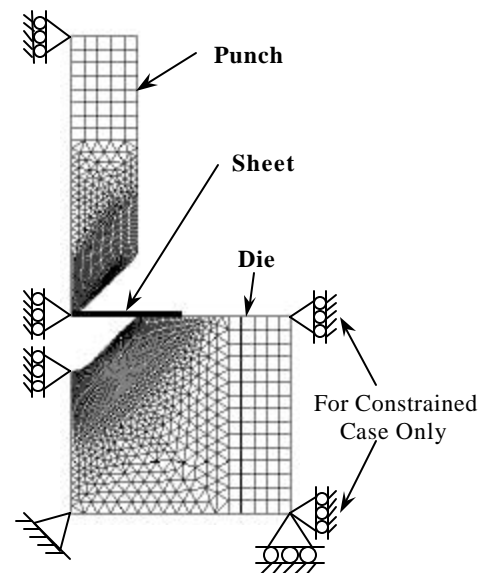
Fig. 4 Finite element model of V-die bending

4   Copyright © 2002 by ASME

determined to be 0.3 mm.

The process simulation consisted of two steps – moving the punch down until it bottoms exactly and returning it to the original position. Since the process involved large, localized deformation and the time increment was kept small relative to the total simulation time, it was treated as a nonlinear static problem. ABAQUS/Standard was used as the solver.

Table 2 V-die bending process parameters

| Process Parameter	A Preliminary FE Model for Validation	B Base FE Model for Parameter Study
Bend radius R_b	5 mm	5 mm
Die shoulder radius R_s	5 mm	5 mm
Die opening W	25 mm	30 mm
Die width W_d	100 mm	100 mm
Die thickness D (into the paper)	8.5 mm	1 mm
Sheet material	3003-H14 Al	1100-O Al
Sheet thickness T	0.8 mm	1 mm
Punch travel distance d_p	9.5 mm	12.5 mm
Punch speed v_p	120 mm/min	120 mm/min
Friction	$\boldsymbol{m}$= 0.2	No friction
Miscellaneous	Plane stress	Plane strain

Model Validation

The simulation results were compared with experimental results to validate the finite element model. Figure 5 illustrates the laboratory-designed experimental setup for sheet metal bending. An Instron Universal Testing System (Model 4466) was used to apply the bending load, and Instron Series IX Software was used for data acquisition. The die set was CNC-machined from Ren Shape 5166. The same process conditions as the preliminary finite element model (column A in Table 2) were applied.

First, the simulated and experimental bending forces were compared with the literature. The bending forces are plotted as functions of bend angle in Fig. 6. The bending force is a function of punch travel. It increases from zero to a maximum and may decrease as the bend is completed. The force then increases sharply as the punch bottoms.

Bending forces can be estimated by assuming that the process is a case of simple beam bending. Then the maximum bending force before bottoming can be expressed as Eq. (4) [17]
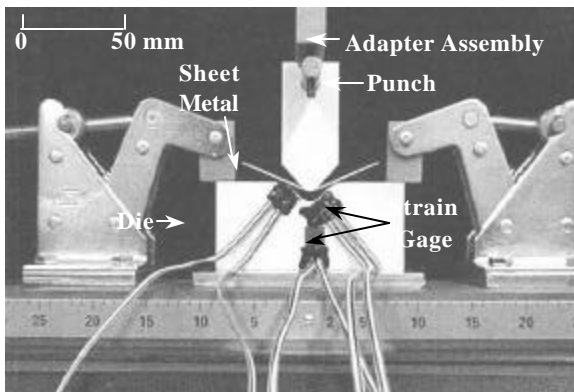
Fig. 5 V-die bending experimental setup
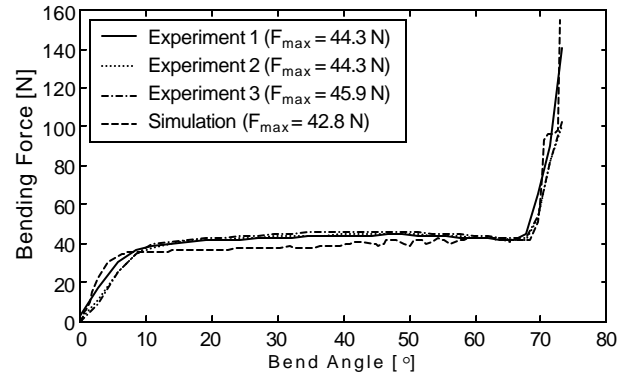
Fig. 6 Comparison of bending forces

$$P_{\max} = k\,\frac{(\mathrm{UTS})LT^2}{W} \qquad (4)$$

where k is die opening factor (1.2 ~ 1.33), UTS is ultimate tensile strength of sheet material, L is length of bend, T is sheet thickness, and W is die opening.

Equation (4) yields the estimated maximum bending force of 41.6 N when $k = 1.2$ is used. (k varies from 1.2 for $W = 16T$ to 1.33 for $W = 8T$.) The simulation and experimental values show good agreement with the estimated value.

Next, a local validation of the finite element analysis results was performed. Three 45° rectangular stacked rosette strain gages were bonded to the die surface at representative points (Figs. 5 and 7), and corresponding strains were measured in the directions as indicated in Fig. 7. Two gages with 0.38 mm gage lengths measured the strains in the bend and die shoulder regions, where strain gradients were large; one gage with a 3.05 mm gage length measured the strains in the bulk region of the die.

As in the finite element model, the punch was allowed to travel until it bottomed exactly, resulting in the maximum bending force of 300 N. The maximum force was appropriate since the corresponding maximum strains were maintained within the allowable range and the limit of the load cell was not exceeded. The elastic strains in the selected directions at the gage locations were collected at this instant and compared with simulated values. In Table 3, the two sets of data show a good agreement, indicating that the finite element model and analysis yield accurate results. Since the gage locations encompass the regions of both high and low strain gradients, the validity of the finite element model can be extended to the entire model.

Table 3 Comparison of strains

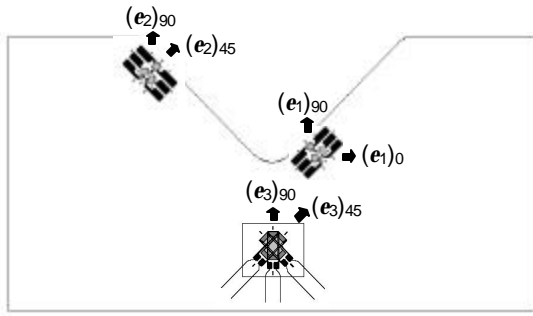| Location	Orientation	Strain [microstrain]	
		Simulated	Experimental
Die bend	$(\boldsymbol{e}_1)_0$	354	395
	$(\boldsymbol{e}_1)_{90}$	-976	-955
Die shoulder	$(\boldsymbol{e}_2)_{45}$	22	25
	$(\boldsymbol{e}_2)_{90}$	-40	-39
Die center	$(\boldsymbol{e}_3)_{45}$	-42	-38
	$(\boldsymbol{e}_3)_{90}$	-71	-83

Copyright © 2002 by ASME

Fig. 7 Strain gage locations and orientations

RESULTS

Parameter Study

To investigate the effect of each parameter on die life, the 'base' finite element model was constructed according to column B of Table 2. As in the previous case, the punch travel distance was set so as to allow exact bottoming. However, a plane strain condition was assumed since it represents a more severe condition than plane stress condition.

First, the effect of die material on the stress field in the die was studied. The punch was not considered since it is subjected to lower stresses as compared to the die in V-die bending. Figure 8 compares the maximum principal stress fields in Ren Shape 5166 and steel dies ($E = 200$ GPa, $n = 0.3$) at the instant the punch bottoms on the die. In both cases, large stress gradients are observed in the 'V' region, whereas stresses are uniformly distributed in the bulk region. Also, deformation remains elastic throughout the process. It should be noted from the magnified views in the bend regions that the steel die exhibits a greater degree of stress concentration due to its higher stiffness. However, the polymer composite die is more prone to crack initiation since its stress level is significantly higher relative to its tensile strength. In other words, under the same process conditions, the stress in the Ren Shape 5166 die is much closer to the tensile strength of the die material than in the case of a steel die.

The effects of parameter variations were studied by varying one parameter at a time in the base model. The parameters under consideration include: (1) geometric parameters, such as bend radius, die shoulder radius, die opening, overall die size (die width), and sheet thickness, (2) material parameters, such as sheet material and friction at punch-sheet-die interfaces, and (3) process parameters, such as
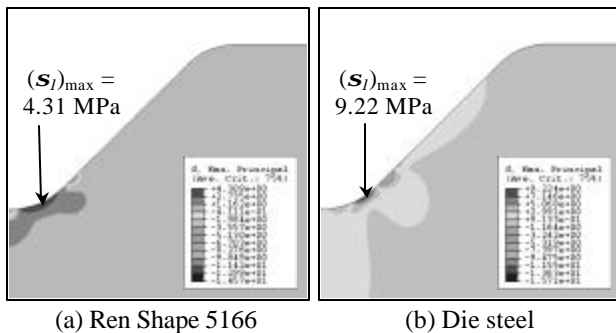

$(s_1)_{max} =$ 4.31 MPa

$(s_1)_{max} =$ 9.22 MPa

(a) Ren Shape 5166   (b) Die steel

Fig. 8 Maximum principal stress fields in the die

punch travel distance and the boundary constraint on the die imposed by the fixture (as illustrated in Fig. 4). The maximum tensile principal stress $(s_1)_{max}$ is used as the output for comparison.

Table 4 shows the sensitivity of the stress state to parameter variations. In all cases, the maximum $(s_1)_{max}$ occurs in the bend area of the die, which tends to act as a stress concentration site, at the bottoming phase.

Table 4 clearly shows that punch over-travel Δd_p (define by the amount punch travels in addition to the distance for exact bottoming) is the most dominant parameter governing the stress state. Referring to the *S-N* data in Fig. 3, in all cases except when Δd_p is greater than 0.2 mm, the die will fail by wear. When Δd_p is 0.25, 0.3, 0.35 mm, Eq. (2) yields the estimated fatigue lives of 7867, 367, 28 cycles, respectively.

Table 4 Effects of parameter variation

Parameter	Value	$(s_1)_{max}$ [MPa]
Bend radius [mm]	3	8.77
	5	4.31
	7	2.54
	10	2.11
Die shoulder radius [mm]	3	4.39
	5	4.31
	7	4.19
	10	4.15
Die opening [mm]	20	3.89
	30	4.31
	40	5.72
	50	6.13
Die width [mm]	80	4.70
	90	4.47
	100	4.31
	110	4.19
Sheet thickness [mm]	0.6	2.95
	1.0	4.31
	1.4	6.82
Friction coefficient	0	4.31
	0.1	3.42
	0.2	3.41
	0.3	3.68
	0.4	4.46
Sheet strength (Yield stress + UTS) [MPa]	125 (1100-O Al)	4.31
	243.3 (Copper)	7.66
	285 (5052-O Al)	9.46
	400 (70-30 Brass)	12.28
Punch over-travel [mm]	0.1	19.10
	0.15	26.11
	0.2	32.03
	0.25	35.67
	0.3	41.42
	0.35	46.26
Die constraint	Unconstrained	4.31
	Constrained	3.98

In addition to punch over-travel, bend radius, sheet thickness, and strength of sheet material, where the strength is represented by the sum of the yield and ultimate tensile strengths, have significant effects on $(s_1)_{max}$. Sheet material

6   Copyright © 2002 by ASME

has a significant influence because even when the punch is bottomed, the sheet, punch, and die surfaces are not in full contact, the configuration depending on the sheet strength. Die opening also has an effect to some degree, but it is not as influential as other parameters. In addition, it can be noted that the critical stress level can be reduced to a certain extent if the outward expansion of the die is constrained – for example, by using an insert-type die or by applying the fixture to the sides of the die.

Size Effect

The size effect was considered to assess the extent of under- or over-estimation of fatigue lives. The 'base' model with $\Delta d_p = 0.35$ mm was chosen. First, a finite element model was created to simulate four-point bending identical to the previous fatigue test mode. When the maximum stress reached 46.26 MPa, V_0 was approximated to be 70 mm^3. Then, the V-die bending model was considered, where V was approximated to be 6 mm^3. From Eq. (3), $S_e/S_{e0} = 1.09$, which implies that the fatigue life might have been slightly under-estimated for this case. In other words, the endurance limit of the die is 9 percent greater than that of the specimen, and the die should last longer than the specimen when the two are subjected to the same maximum stress.

Although the die has a larger volume than a fatigue test specimen, the volume of the die experiencing the maximum stress ($V = 6$ mm^3) is significantly smaller than that of the specimen ($V_0 = 70$ mm^3), since the bend radius in the die acts as a notch. From a statistical viewpoint, the smaller the critically stressed volume, the smaller the probability of finding a defect, which would lead to more rapid failure.

Wear Considerations

Die wear was taken into account by performing V-bending experiments until the die failed by fatigue and by examining the die for any sign of wear. In order to accommodate the load frame and load cell capacity, the conditions in column A of Table 2 were used except for the following: $W = 30$ mm, $D = 10$ mm, and $T = 1$ mm. Bend radii of 3 mm and 5 mm were applied, and in each case, the punch travel distance was
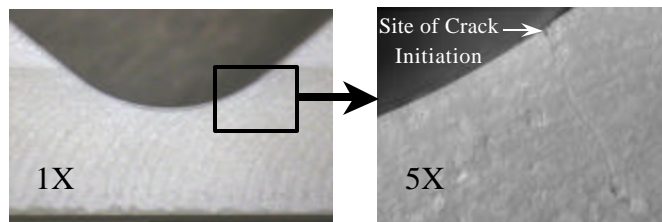
(a) After 5000 stamping cycles ($R_b = 5$ mm)
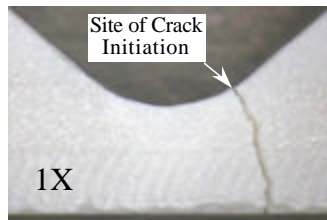
(b) After 507 stamping cycles ($R_b = 3$ mm)

Fig. 9 Fatigue failure of V-bending dies

selected such that the maximum bending force was limited to 8 kN.

Figures 9(a) and 9(b) show the 'V' regions of the dies after fatigue failure has been reached. The die with a 5 mm bend radius lasted for 5000 cycles while that with a 3 mm bend radius lasted for 507 cycles. This clearly shows that a sharper bend radius causes the die to be subject to fast crack propagation and stress concentration. A microscopic examination of the die surfaces that contacted the sheet metal revealed no sign of wear. High compressive strength and wear resistance of Ren Shape 5166 drives the die to fail by fatigue in V-bending. However, wear may become an issue if the normal load and the relative sliding velocity between the die and the sheet metal are high.

CONCLUSION

In this paper, a method was presented to estimate the fatigue life of a sheet metal forming die fabricated from ATH-filled polyurethane. First, engineering data were obtained by characterizing the material in various perspectives – microstructure, mechanical behavior, and tribological properties. Then, on the basis of material data, a finite element method was employed to obtain the stress distribution in the die. In the proposed local stress-based fatigue approach, the stress levels at critical regions serve as the indices for determining the cycles to fatigue failure. Furthermore, the finite element method was used to investigate the effects of process parameters on the fatigue life of the die. The next step of the research is to validate the die prediction method experimentally.

The proposed method can be applied to a general polymer composite tooling material for metal forming, where the plasticity of the die is negligible. When a new tooling material is introduced, the first step is to determine the failure mode of the die, *i.e.* the dominance of plasticity. If plasticity is not negligible, it is suggested that a strain-based fatigue approach be used with von Mises stress as the criterion. Also, the number of cycles expended in crack propagation as well as initiation may have to be considered.

The proposed approach can be extended to other sheet metal forming processes that involve more complex geometry and mechanics, such as deep drawing. The presented parameter study lays the groundwork for providing reliable tool life prediction and design optimization guidelines for advanced polymer tooling materials in metal forming.

REFERENCES

1. Mishek, J., "Rapid Prototyping Tests Point to its Uses and Drawbacks," Vista Technologies LLC Publications (www.vistatek.com).
2. Nakagawa, T., 2000, "Advances in Prototype and Low Volume Sheet Forming and Tooling," Journal of Materials Processing Technology, **98**, pp. 244-250.

3. Miller, W., 1999, "Producing Dies for Rapid Prototyping of Metal Formed Parts," The Fabricator, **29**, No. 4.

4. Altan, T., and Vazquez, V., 1996, "Numerical Process Simulation for Tool and Process Design in Bulk Metal Forming," CIRP Annals, **45**, No. 2, pp. 599-615.

5. Knoerr, M., Lange, K., and Altan, T., 1994, "Fatigue Failure of Cold Forging Tooling: Causes and Possible Solutions through Fatigue Analysis," Journal of Materials Processing Technology, **46**, pp. 57-71.

6. Geiger, M., Hansel, M., and Rebhan, T., 1992, "Improving the Fatigue Resistance of Cold Forging Tools by FE Simulation and Computer Aided Die Shape Optimization," IMechE, Part B: Journal of Engineering Manufacture, **206**, pp. 143-150.

7. Falk, B., Engel, U., and Geiger, M., 1998, "Estimation of Tool Life in Bulk Metal Forming Based on Different Failure Concepts", Journal of Materials Processing Technology, **80-81**, pp. 602-607.

8. Jensen, M. R., Damborg, F. F., Nielsen, K. B., and Danckert, J., 1998, "Applying the Finite-Element Method for Determination of Tool Wear in Conventional Deep-Drawing," Journal of Materials Processing Technology, **83**, pp. 98-105.

9. Ratner, S. B., and Potapova, L. B., 1991, "Multicycle Fatigue Resistance of Brittle Polymers," Mechanics of Composite Materials, **26**, No. 4, pp. 463-467.

10. Suresh, S., 1998, *Fatigue of Materials*, Cambridge University Press, Cambridge, UK.

11. Ritchie, R. O., Gilbert, J. M., and McNaney, J. M., 2000, "Mechanics and Mechanisms of Fatigue Damage and Crack Growth in Advanced Materials," International Journal of Solids and Structures, **37**, No. 1, pp. 311-329.

12. Tadmor, Z., and Gogos, C. G., 1979, *Principles of Polymer Processing*, John Wiley and Sons, New York, NY.

13. Bannantine, J. A., Comer, J. J., and Handrock, J. L., 1990, *Fundamentals of Metal Fatigue Analysis*, Prentice Hall, Englewood Cliffs, NJ.

14. Hertzberg, R. W., 1996, *Deformation and Fracture Mechanics of Engineering Materials*, John Wiley and Sons, New York, NY.

15. Kuguel, R., 1961, "A Relationship between Theoretical Stress Concentration Factor and Fatigue Notch Factor Deduced from the Concept of Highly Stressed Volume," American Society for Testing and Materials Proceedings, **61**, pp. 732-748.

16. American Society of Tool and Manufacturing Engineers, 1965, *Die Design Handbook*, McGraw-Hill, New York, NY.

17. Kalpakjian, S., 1997, *Manufacturing Processes for Engineering Materials*, Addison-Wesley, Menlo Park, CA.